TITLE

Antisense transcription interferes with heterologous expression of a codon-optimised mNeonGreen fluorescent reporter in the chloroplast of *Chlamydomonas reinhardtii*.

Axel Navarrete[1] & Bernardo Pollak[1,2,*].

[1] Instituto Milenio de Biología Integrativa (iBio), Santiago, Chile.

[2] Fundación Ciencia y Vida, Santiago, Chile.

[*]Corresponding author

Email address: bpollakw@gmail.com

ABSTRACT

Although over 30 years have passed since *Chlamydomonas reinhardtii* chloroplast transformation was first achieved, genetic engineering of the chloroplast still remains an arduous task. The glass-bead transformation method has enabled simple and accessible chloroplast transformation of the *C. reinhardtii* TN72 strain, allowing generation of marker-free transplastomic strains for low-cost experimentation. However, lack of functional fluorescent reporters limit research and widespread development of chloroplast engineering. Here, we developed a codon-optimised mNeonGreen fluorescent reporter, which can be detected *in vivo* through fluorometry and microscopy. We found evidence for chloroplast post-transcriptional regulation of gene expression derived from formation of antisense pairing of mRNAs due to readthrough of convergent adjacent genes. In addition, synthetic biology approaches were used to modulate transcriptional readthrough, allowing a better understanding of context effects relevant for heterologous expression. This work provides new tools to study basic aspects of the molecular biology in the chloroplast in *C. reinhardtii*, as well as evidence for fundamental processes of gene regulation that may enable developing rules for more efficient chloroplast engineering.

KEYWORDS

Chlamydomonas, chloroplast, fluorescent reporter, mNeonGreen, transcriptional readthrough, antisense RNA, dsRNA.

INTRODUCTION

Chloroplast transformation was first achieved by biolistics [Boynton et al., 1988] [Svab et al., 1990], and is considered the most effective way for delivering DNA into plastids because of its high efficiency. However, high costs of biolistics restricts chloroplast research to well-funded laboratories and limits accessibility. A low-cost chloroplast transformation method using glass beads was developed for *C. reinhardtii* [Kindle et al., 1991] and further optimized by the use of cell wall-deficient strains, which may be used directly without prior digestion of its cell wall [Young and Purton, 2014]. This method, along with the use of complementation of an insertional mutant of psbH coding for the photosystem II reaction center protein H in the TN72 strain, enables generation of marker-free transplastomic *C. reinhardtii* strains [Wannathong et al. 2016], providing an accessible platform for chloroplast research.

Fluorescent reporters excel in providing detailed spatial and temporal information for the observation of dynamical processes at the cellular and molecular level. Despite substantial progress in the study of the chloroplast's biology, fluorescent proteins have not been successfully used as reporters in the *C. reinhardtii* chloroplast. Conflicting evidence has been presented for their poor performance as a reporter, where presence of gene transcripts and protein has been shown but observation of fluorescence through microscopy has been challenging, suggesting that chlorophyll autofluorescence may impede fluorescent reporter visualization [Franklin et al. 2002] [Braun-Galleani et al. 2015]. In contrast, efforts using nuclear-encoded chloroplast-localized proteins have been undertaken [Karcher et al. 2009] [Lauersen et al. 2015] [Crozet et al. 2018], suggesting that reporter fluorescence is not an issue in the chloroplast, but rather the post-transcriptional gene regulation of the chloroplast-encoded reporters.

Chloroplasts contain prokaryotic and eukaryotic transcriptional machinery, allowing expression of multiple genes as polycistronic transcripts, as well as possessing RNA regulated by cis- and trans- splicing [Stern et al., 2010] [Barkan, 2011]. Transcription in the chloroplast of Chlamydomonas is performed by a plastid-encoded RNA polymerase (PEP), and aspects of regulatory mechanisms governing transcriptional termination are gaining attention [Ji et al., 2019]. The chloroplast genome shows pervasive genome-wide transcription [Shi et al., 2016], with inefficient mechanisms for transcriptional termination [Rott et al., 1996], highlighting the

importance of RNA degradation in the chloroplast [Schein et al. 2008]. New evidence has shown that transgene insertion in the chloroplast can have disruptive effects for native chloroplast genes in the context of insertion [Ghandour et al. 2023]. Transgene insertion can result in antisense readthrough from adjacent genes, which has been suggested to create untranslatable double-stranded RNA [Rochaix et al., 1991] [Prikryl et al., 2010]. These reports underscore the need to gain deeper understanding into the biology of chloroplasts, as well as context-aware strategies for more efficient chloroplast engineering.

Available vectors for chloroplast transformation of the TN72 strain, such as the pASapI and derivatives, reestablish the *psbH* functionality and enable expression of a single GOI in an antisense orientation with *psbH* [Braun-Galleani et al. 2015] [Young et al. 2016]. The architecture of these constructs has been used for expression of recombinant proteins as well as reporter proteins, but observation of fluorescent proteins through microscopy was not reported [Braun-Galleani et al. 2015] [Kim et al. 2020]. Limited flexibility of these vectors restrict evaluation of effects of transgene orientation for heterologous expression.

A system based on Golden-Gate cloning was developed for *C. reinhardtii* chloroplast expression [Bertalan et al., 2015]. This system allows modification of regulatory elements, but is tethered to a specific recombination locus and is not interoperable with the Common Syntax for Standard Parts [Patron 2015]. Additionally, a modular cloning toolkit for chloroplast biotechnology in higher plants was developed [Occhialini et al., 2019], containing chloroplast regulatory elements, codon-optimized coding sequences for chloroplast expression, and destination vectors suited for chloroplast transformation of *Nicotiana tabacum*, *Zea mays*, and *Solanum tuberosum*. The issue of host-specific requirements for transformation has been approached through the Universal Loop (uLoop) assembly [Pollak et al., 2020]. This system has enabled higher flexibility to develop constructs for species-agnostic transformation by decoupling elements required for host transformation and has been used in bacteria, yeast, plants, diatoms and cell-free systems [Pollak et al., 2020] [Taparia et al., 2022] [Moosburner et al. 2022] [Arce et al. 2021]. Moreover, uLoop parts are interoperable with assembly systems that use the Common Syntax, and its versatility could enable exploring of multiple sequence combinations and their implications for transgene expression in the chloroplast of *C. reinhardtii*.

In this work, we developed vectors for *C. reinhardtii* TN72 chloroplast transformation that enable efficient mNeonGreen reporter expression observable through microscopy. Different vector designs were tested that included changes in orientation of selectable gene and reporter gene, showing that readthrough transcription disrupts expression of the fluorescent reporter when placed in an antisense orientation with *psbH*. *psbH* evidenced context effects affecting mNeonGreen fluorescence levels due to transcriptional readthrough of both genes. Confirmation of autonomous *mNG* transcripts allowed combinatorial approaches of both endogenous and heterologous cis regulatory elements in the reporter gene, which were evaluated under different culture conditions to identify functional and efficient combinations for chloroplast expression. Subcellular localization of the fluorescent reporter protein was identified, enabling observation of ultrastructural details by multispectral confocal microscopy.

RESULTS

A modular vector system using uLoop was developed based on the pASapI vector [Wannathong et al., 2016] for chloroplast transformation of *C. reinhardtii* (Figure S1). These vectors, the pLCh series, consisted of four modules including an upstream recombination element, a fluorescent reporter, psbH transcription unit as a selection marker, and a downstream recombination element. Although the initial pLCh0 design failed, suggesting issues with the psbH selection marker placed in the opposite direction as its genome copy, subsequent vectors, pLCh1 and pLCh2, demonstrated successful integration (Figure S2a) and comparable transformation rates to the original pASapI vector. Additionally, they exhibited no significant differences in growth rate or transformation efficiency (Figure S1cd), rendering them suitable for further experimentation.

Fluorescent protein expression in chloroplast of *C. reinhardtii*.

To evaluate pLCh vectors capability to generate transplastomic strains that express an heterologous gene in the chloroplast, pLCh1 and pLCh2 vectors were used to generate constructs encoding the fluorescent reporter gene mNeonGreen (*mNG*). The regulatory sequences used to drive expression of *mNG* were similar to the elements present in pASapI. Three pLCh vectors were generated by modular assembly: a) a pLCh1 vector with the reporter expression driven by the *atpA* promoter (PatpA) and its 5'UTR [Ishikura et al. 1999]; a *mNG* CDS that was codon-optimized for chloroplast expression in *C. reinhardtii* (*Cr*Cp), in addition to the C-terminal segment of *rbcL* coding sequence and the *rbcL* 3'UTR and terminator (pLCh1-*mNG::Ct-RbcL*) [Wannathong et al. 2016]. These elements, except for *mNG Cr*Cp CDS, were the same as the ones in the pASapI vector for the GOI. b) a pLCh1 vector similar to the previously mentioned, but excluding the C-terminal segment of *rbcL* gene (pLCh1-*mNG*). c) a pLCh2 vector with the same reporter gene but without the C-terminal segment of the *rbcL* coding sequence (pLCh2-*mNG*). In addition, a pLCh2-empty vector was used as fluorescence negative control and the four vectors were used for chloroplast transformation of the *C. reinhardtii* TN72 strain. After confirming homoplasmicity (Figure S2b), newly obtained transplastomic strains were observed by epifluorescence microscopy and their *in vivo* fluorescence intensity was measured by microplate fluorometry.

138 Epifluorescence microscopy revealed a high signal in the mNG channel of LCh2-*mNG* strains,
139 which could not be seen in other strains (Figure 1a and 1b). This signal also showed
140 co-localization with chloroplast fluorescence visualized in the chlorophyll channel (Figure 1a).
141 Fluorescence intensity values obtained by *in vivo* fluorometry in transformants obtained with the
142 pLCh1-*mNG::CtRbcL* and pLCh1-*mNG* vectors presented no significant differences compared to
143 the negative control, but fluorescence levels of strains obtained by chloroplast transformations
144 using the pLCh2-*mNG* vector showed significant differences compared to the negative control
145 and LCh1 strains. LCh2-*mNG* strains fluorescence values (~53000 RFU) were ~6-fold higher
146 than the other strains (~9000 RFU) (Figure 1b).
147
148 **Effects of the *psbH* terminator in reporter fluorescence levels.**
149 pLCh designs used for transgene integration into the chloroplast genome used two transcriptional
150 units adjacent to each other, the reporter and *psbH*. Recent transcriptomic analysis of *C.*
151 *reinhardtii* chloroplast transcripts revealed that vector designs used for transgene integration in
152 the psbH locus use an incomplete *psbH* 3'UTR terminator sequence (T*psbH//*) [Gallaher *et al*.
153 2018]. Due to this, different terminator sequences were tested to replace the incomplete 3'UTR
154 terminator sequence used in the *psbH* selection gene to evaluate transcription conditions of the
155 psbH selectable gene and the reporter gene in strains transformed with pLCh2 vectors (Figure
156 2a), and were subsequently compared with LCh1-*mNG* and LCh2-*mNG* stains. Four 3'UTR
157 terminator sequences from different species were tested as terminators for *psbH* in pLCh2
158 vectors using the same mNG reporter as in pLCh2-*mNG*, and transformants obtained using the
159 pLCh2-*mNG* vector were used as fluorescence control.
160
161 Transformant colonies were compared among different constructs used, and T*psbA* (*Nt*Cp) and
162 T*tmv* terminators for psbH sequences presented similar transformation efficiency when
163 compared to transformations using the pLCh2-empty vector, and showed improved efficiency
164 compared to the positive control. This did not occur with vectors containing T*rbcL* and T*rrnB*
165 (*Ec*) sequences. Notably, transformations with vectors containing T*psbA* (*Nt*Cp) and T*tmv*
166 sequences presented transformant colonies the first week after transformation (Figure 2b).
167
168 After homoplasmicity confirmation of transformed strains (Figure S2c), *in vivo* fluorescence

levels of *C. reinhardtii* liquid cultures grown under different conditions were measured by microplate fluorometry, and only strains grown in photoautotrophic growth condition were observed through epifluorescence microscopy. Fluorometry results showed that fluorescence levels in positive control strains presented the highest fluorescence intensity among all strains in every growth condition, showing an increase of ~50% in fluorescence signal under mixotrophic and heterotrophic conditions (TAP-L and TAP-D, respectively) compared to photoautotrophic conditions (HSM) (Figure 2c). Strains containing terminators different than T*psbH//* in the selection gene presented lower fluorescence levels than control strain in all conditions, with strains using the T*psbA* (*Nt*Cp) and T*tmv* termination sequences showing ~30% less compared to control strains, followed by strains with T*rrnB* (*Ec*) sequence with reduction of ~70% of their fluorescence levels; and finally, strains with T*rbcL* (*Cr*Cp) presented no significant differences regarding to negative control strains in any of the culture conditions (Figure 2c). Notably, the positive control maintained high fluorescence levels in heterotrophic conditions, while in the same condition, strains with terminator sequences different than T*psbH//* presented the lowest fluorescence intensity among all conditions.

Fluorescence intensity detected through epifluorescence microscopy was in agreement with the results obtained by fluorometry (Figure 2d). As in positive control strains, strains with terminator sequences different than T*psbH//* showed fluorescent signal in the mNG channel, with exception of strains containing T*rbcL* sequence, which presented barely any fluorescence. Fluorescent signals in the mNG channel from strains containing T*psbA*, Ttmv and T*rrnB* also showed co-localization with chloroplast autofluorescence in the Chl channel.

Transcriptional readthrough of *psbH* and *mNG* in sense and antisense orientation and effects on fluorescent reporter expression in the chloroplast of *C. reinhardtii*.

To evaluate underlying causes for the effects observed from the psbH terminator on reporter gene expression, semiquantitative RT-PCR was performed to find evidence of transcriptional readthrough occurring in *psbH* and *mNG*. Using specific primers for cDNA synthesis through reverse transcription of total RNA from a representative strain of every different transplastomic strain, unterminated transcripts derived from *psbH* and *mNG* transcription were evaluated (Figure 3a). Agarose electrophoresis showed that readthrough of *psbH* (R1 and R2) up to *mNG*

CDS (*psbH-mNG*) was detected in all strains except in negative control (Figure 3b). On the other hand, transcripts of *mNG* were detected in both LCh1 and LCh2 strains, but not in the negative control. In addition, readthrough of *mNG* (*mNG-psbH*) up to the *psbH* CDS (R3v2) was detected in the LCh1 strain, but not in the negative control and the LCh2 strain (Figure 3c).

After confirming the presence of readthrough in *psbH* transcripts, *psbH-mNG* readthrough transcript levels and total *mNG* transcript levels were analysed by absolute quantification through RT-qPCR. Significant differences between the amount of *psbH-mNG* readthrough and total *mNG* transcripts can evidence the presence of autonomous *mNG* transcripts, due to that total amount of *mNG* transcripts includes *psbH-mNG* readthrough and autonomous *mNG* transcripts as well (Figure 3d). Absolute quantification of total *mNG* transcripts showed significant differences when compared to *psbH-mNG* readthrough transcripts in LCh2 strains with T*psbH//* (LCh2-*mNG*), T*rbcL* and T*tmv* 3'UTR + terminator sequences, with copies/ng RNA of total *mNG* transcripts being ~5-fold higher than *psbH-mNG* readthrough transcripts in the case of the LCh2-*mNG* and T*tmv* strains. This difference in total *mNG* transcripts was ~100-fold higher than *psbH-mNG* readthrough transcripts in the T*rbcL* strains, but total *mNG* transcript level was ~100-fold lower than in the LCh2-*mNG* strains. Statistical analyses showed there were no significant differences between *psbH-mNG* readthrough transcripts and total *mNG* transcripts in T*psbA* (*Nt*Cp) and T*rrnB* (*Ec*) strains.

To evaluate translation of the *mNG* transcripts, total protein extracts were obtained and used in native polyacrylamide gel electrophoresis (native-PAGE) to confirm protein presence by fluorescence visualization (Figure 3e). Gel exposure to blue light evidenced that there was mNG presence in protein extracts from LCh2-*mNG*, T*psbA*, T*tmv* and T*rrnB* strains, with no evidence of mNG in extracts from LCh2-empty, LCh1-*mNG* and T*rbcL* (*Cr*Cp) strains. After fluorescence visualization, the gel was stained with Coomassie Blue, which caused loss of mNG fluorescence signal but showed similar amounts of total protein loaded in each well. No migration pattern differences were observed among the samples, nor specific bands for the mNG protein was identified by Coomassie Blue gel staining.

Characterisation of regulatory elements through reporter fluorescence levels in the chloroplast of *C. reinhardtii.*

After confirming the presence of autonomous *mNG* transcripts in transplastomic strains, characterisation of different promoters, 5'UTR and 3'UTR terminator sequences from different sources was performed in order to find combinations for efficient fluorescent reporter expression in the chloroplast. The pLCh2 vector design using the *psbH* selectable gene with the *tmv* 3'UTR termination sequence was used for this experiment, altering only regulatory elements in the *mNG* reporter (Figure 4a). Modifications of the regulatory elements in this experiment consisted in replacing a single element per construct (either promoter, or 5'UTR or 3'UTR terminator) using the P*atpA*-*mNG*-T*rbcL* transcription unit as control (Figure 4b). Constructs were used for chloroplast transformation and strains were cultured in photoautotrophic (HSM), mixotrophic (TAP-L) and heterotrophic (TAP-D) conditions were evaluated by fluorometry after confirmation of homoplasmicity (Figure S2d).

Changes to the regulatory sequences of the *mNG* transcription unit showed increased fluorescence levels for strains containing T*rrnB* (*Ec*) (pLCh2-D), P*rrnS* (*Cr*Cp) (pLCh2-E), and P*rrnS* (*Cr*Cp) + *psbA* 5'UTR (*Cr*Cp) (pLCh2-F) sequences. Particularly, the pLCh2-E construct showed a ~2-fold increase in fluorescence levels of strains under phototrophic and mixotrophic conditions compared to the control. Furthermore, the LCh2-F strains displayed comparable fluorescence levels to LCh2-E strains in mixotrophic and heterotrophic cultures, but under phototrophic conditions showed lower fluorescence.

Both LCh2-E and LCh2-F strains stood out as the only strains incorporating endogenous regulatory sequences, apart from the control. The LCh2-G strain, which resembled the pLCh2-F design but featured the *Nicotiana tabacum* chloroplast version of *psbA* 5'UTR, showed a 33% decrease of fluorescence compared to the control in photoautotrophic conditions.

In other constructs, replacing the T*rbcL* (*Cr*Cp) 3'UTR terminator sequence with T*rcbL* (*Nt*Cp) resulted in approximately 50% less fluorescence of strains in photoautotrophic conditions (LCh2-B). Additionally, strains resulting from the replacement of T*rbcL* (*Cr*Cp) with T*rnnB*

(*Ec*), exemplified by LCh2-D, demonstrated functionality and stable fluorescence levels in all culture conditions compared to the control.

Transformations using heterologous promoter sequences alongside a replacement of the *atpA* 5'UTR (*Cr*Cp) by *psbA* 5'UTR (*Cr*Cp), similar to LCh2-F strains, showed decreased fluorescence levels in the LCh2-H strain using the P*psbA* (*Nt*Cp) under all conditions. However, the LCh2-I and LCh2-J strains, employing P*rbcL* (*Nt*Cp) and P*rpoB* (NtCp) sequences respectively, only showed a 50% and a 62% decrease in fluorescence under photoautotrophic conditions.

Fluorescent reporter subcellular localization and ultrastructure imaging of *C. reinhardtii* chloroplast.

Subcellular localization of fluorescent reporter protein was assessed in chloroplasts of *C. reinhardtii* using confocal microscopy. LCh2-*mNG* strains were stained with DAPI and optical sections in different z-axis planes were obtained through laser excitation and collection of fluorescence for independent channels assigned as Chl for chlorophyll autofluorescence, mNG for reporter protein, and DAPI for nuclear content. Microscopy images showed presence of mNG fluorescence inside the chloroplast of *C. reinhardtii*, not strictly colocalized with chloroplast autofluorescence but with an heterogeneous distribution (Figure 5a, progressions 3-4) and also specific optical sections showed exclusion from cylindrical structures (Figure 5a, progression 1), with most of the signal presumably occupying the stroma of the chloroplast. A greater accumulation of mNG fluorescence was observed in the center of chloroplast lumen, with the highest green signal presumably located in the zone where pyrenoid is located (Figure 5a, progressions 3-4). Notably, most of the mNG fluorescence signal does not co-localize with chloroplast fluorescence.

Using three dimensional reconstructions with orthogonal images, we were able to confirm mNG localization inside the chloroplast. In the XZ and YZ focal planes (Figure 5b), it is possible to distinguish DAPI cytosolic signal (blue) excluded from chloroplast autofluorescence (red), with mNG fluorescence (green) distributed among the chloroplast signal, concentrating its accumulation inside the red signal limits and presumably in the pyrenoid periphery.

291

292 **DISCUSSION**

293

294 This study describes the development of uLoop-based vector designs that allowed the evaluation
295 of different insertion unit configurations in the *C. reinhardtii* TN72 strain. The use of uLoop
296 overcame the limitations of traditional molecular cloning systems by enabling alterations in
297 selectable markers, recombination elements, and the regulatory sequences of reporter and
298 selectable marker. Furthermore, it is interoperable with other modular cloning systems that use
299 the Common Syntax, which enabled using available chloroplast heterologous regulatory
300 elements for characterisation. Despite encountering challenges with recovery of photoautotrophy
301 when altering the orientation of the *psbH* transcription unit, the study underscored the potential
302 of the uLoop system in chloroplast research, particularly its capacity to explore molecular
303 mechanisms, study heterologous elements for gene expression, and scrutinize transcriptional and
304 post-transcriptional events in the chloroplast of *C. reinhardtii*.

305

306 **Efficient protein production by using pLCh2 vectors for chloroplast transformation of *C.***
307 ***reinhardtii*.**

308 mNeonGreen fluorescence was successfully detected through *in vivo* fluorimetry and
309 epifluorescence microscopy in transplastomic strains transformed with pLCh2 vectors. Several
310 attempts have been undertaken to use fluorescent protein genes as reporters in the chloroplast of
311 *C. reinhardtii* [GFP, Franklin et al. 2002] [VFP, Braun-Galleani et al. 2015] [mCherry, Kim et al.
312 2020] [Venus, Jackson et al 2022]. These studies describe fluorescent protein presence, but lack
313 evidence showing fluorescent cells using imaging methods, which is attributed to quenching of
314 the absorption capacity of fluorescent reporters by chlorophyll autofluorescence [Franklin et al.
315 2002] [Rasala et al. 2013]. In contrast, other works show efficient fluorescence from
316 nuclear-encoded chloroplast-localized fluorescent proteins [Crozet et al. 2018] [Lauersen et al.
317 2015] [Karcher et al. 2009], suggesting that chloroplast-encoded fluorescent reporters may have
318 low expression or that more sophisticated strategies are required to ensure detection
319 [Noor-Mohammadi et al., 2012] [Fields et al. 2019]. In this work, we used a *C. reinhardtii*
320 chloroplast codon-optimised version of mNeonGreen (*mNG*) [Shaner et al. 2013], since it
321 absorbs and emits light in a range that is mostly out of the range of chlorophyll autofluorescence,

322 and due to its fluorescence intensity as it is the brightest monomeric fluorescent protein reported
323 to date. The use of pLCh1 vectors recapitulates a transformation event with a pASapI vector due
324 to the identity of their regulatory elements composition, and the mNG fluorescence signal of
325 strains obtained using this vector did not present significant differences compared with negative
326 control strains. However, the change in orientation of the transcriptional unit made in pLCh2
327 vectors enabled detection of mNG through fluorometry and epifluorescence microscopy, which
328 suggests issues with transcriptional/post-transcriptional events rather than events related to
329 protein biology in LCh1 strains.
330
331 **Transcriptional readthrough of both selectable gene and reporter gene affects reporter**
332 **protein accumulation in the chloroplast of *C. reinhardtii* LCh1 strains.**
333 Experiments to determine transcriptional readthrough of *psbH* showed that it is pervasive, being
334 present in both LCh1 and LCh2 strains. Chloroplast transcription is known to enable
335 polycistronic expression due to its prokaryotic origin [Barkan, 2011], and while *psbH*
336 transcriptional readthrough in LCh1 is likely to create a dsRNA through asRNA pairing with
337 *mNG* readthrough encoded in the opposite strand, in LCh2 it would generate a bi-cistronic
338 transcript that includes *psbH* and *mNG*. Formation of antisense pairs between both transcription
339 units, would result in formation of dsRNA, which may interfere with translation and can explain
340 absence of *in vivo* fluorescence in LCh1-*mNG* strains despite confirming presence of *mNG*
341 mRNA. Formation of dsRNA may also impede the fluorescent reporter protein detection through
342 methods used in this work, but not for high sensitivity methods described in other works such as
343 protein immunoblot [Franklin et al. 2002] [Braun-Galleani et al. 2015]. A similar situation has
344 been reported in adjacent convergent genes being expressed in *N. tabacum* chloroplasts, where
345 GFP could only be detected by protein immunoblot, probably due to lack of fluorescence signal
346 [Tangphatsornruang et al. 2010]. In addition, translation of *psbH* mRNA might not be impeded
347 by antisense pairing due that *psbH* is the selectable gene for this strain, being required for cell
348 viability under photoautotrophic culture conditions.
349
350 Mechanisms including post-transcriptional regulation are described to occur in chloroplasts
351 [Schein et al. 2008] [Kishine et al. 2004] [Sharwood et al. 2011]. Among these, Ribonuclease J is
352 one of the major mRNA degradation pathways in prokaryotes, and it has been the only

353 ribonuclease identified to have a role in the chloroplast of *C. reinhardtii* [Liponska et al. 2018]. It
354 has been hypothesized that after an endonuclease cleavage of dsRNA, probably performed by the
355 same enzyme, exoribonuclease activity of ribonuclease J may allow degradation of dsRNA 5'
356 ends, which may prevent accumulation of dsRNA derived from sense and antisense transcription
357 [De La Sierra-Gallay et al. 2008]. Inefficient transcriptional termination in the chloroplast of *C.*
358 *reinhardtii* may cause difficulties in translation of transcripts that are convergently located in
359 opposite strands. In prokaryotes, antisense RNA can repress translation by sequestering
360 Shine-Dalgarno elements or other regulatory motifs [Waters and Storz 2009]. In chloroplasts,
361 translation of transcripts can also be impeded when 5'UTR sequences are engaged in
362 double-stranded structures, which can be relieved through binding of translation activation
363 factors [Rochaix et al. 1989] [Prikryl et al. 2010].
364
365 **Substitution of *psbH* terminator in LCh2 strains modulates its transcriptional readthrough.**
366 As an attempt to avoid transcriptional readthrough of *psbH*, different terminators were used as
367 replacement of the *psbH* interrupted terminator in LCh2 transformants. Transformant colonies
368 obtained demonstrate that this sequence might not be essential in the recombination event related
369 to *psbH* UFE as described by pASapI's annotation map. This, together with results obtained by
370 chloroplast transformations using the pLCh0 vector, suggests that sequences required for
371 homologous recombination should be present from *psbH* promoter sequence, including
372 downstream sequences up to early bases of psbH CDS, and before *aadA* gene insertion into the
373 TN72 chloroplast genome. Absolute quantification of transcripts by RT-qPCR allowed us to
374 determine that terminators tested in this work could not completely avoid transcriptional
375 readthrough of *psbH*, supporting the idea that readthrough is pervasive in the chloroplast of *C.*
376 *reinhardtii* [Rott et al., 2022]. Despite this, strains with *psbH//* (LCh2-*mNG*), *rbcL* and *tmv*
377 termination sequences in *psbH* presented significant differences between readthrough and total
378 *mNG* transcript levels, the latter including *mNG* contained in readthrough transcripts and
379 autonomous *mNG* transcripts. T*psbH//* and T*rbcL* are endogenous 3'UTR termination sequences
380 from *C. reinhardtii* chloroplast, which may contribute to termination specificity for
381 transcriptional units whose promoter sequences enable transcription through nuclear-encoded
382 polymerases (NEP) and plastid encoded polymerases (PEP), but the lack of 633 bp in the 3' end
383 of the *psbH* 3'UTR terminator could lead to a decrease in *psbH* termination efficiency, resulting

384 in higher rates of readthrough transcripts than T*rbcL*. Despite the highly reduced *psbH-mNG*
385 transcriptional readthrough compared with other strains, T*rbcL* strains exhibited the lowest
386 mRNA and protein accumulation levels, indistinguishable from negative control strains. This
387 might be due to consecutive use of the same sequence for different consecutive transcriptional
388 units, as the *mNG* reporter also contained T*rbcL* at its 3' end [Larrea-Alvarez and Purton, 2020].
389 In the case of T*psbA* (*Nt*Cp) sequence, it has been described to have a single hairpin structure
390 and to act as regulator of mRNA transcription by interacting with 5'UTR, which seems to highly
391 increase mRNA stability [Katz and Danon 2002]. It is also known that chloroplast 3'UTR
392 sequences improve stability of mRNA through protein interaction with secondary structures, but
393 these mRNA structures are not required for efficient transcription termination [Stern et al. 1987]
394 [Manavski et al. 2018]. The T*tmv* 3'UTR termination sequence consists of a 190 bp sequence
395 that contains domains which form pseudo-knot tRNA-like structures (TLS) [Van Belkum et al.
396 1985] [Osman et al. 2000]. These structures may increase mRNA stability by avoiding 3'
397 exonuclease degradation of *psbH* mRNA [Sharwood et al. 2011]. The *E. coli* T*rrnB* sequence is
398 a strong terminator containing two domains that form hairpins for factor-independent
399 transcription termination [Brosius et al., 1981] [Orosz et al., 1991]. Despite this, there were no
400 significant differences between *psbH-mNG* readthrough and total *mNG* transcripts in these
401 strains, which could suggest that secondary structures do not contribute substantially to
402 transcription termination in *C. reinhardtii* chloroplast.
403
404 Differences were found for transcript levels of LCh2-*mNG*, T*psbA*, T*tmv* and T*rrnB* strains
405 compared with their fluorescence levels detected by fluorometry, epifluorescence microscopy
406 and native-PAGE. This might be attributed to transcript stability and half-life, but previous
407 studies have shown that there is no strict correlation between mRNA levels and protein levels in
408 the chloroplast of *C. reinhardtii* [Eberhard et al. 2002] [Rasala et al. 2011].
409
410 **Characterisation of endogenous and heterologous regulatory elements through fluorescent**
411 **reporter expression in chloroplasts of *C. reinhardtii*.**
412 Characterisation of regulatory elements for driving the expression of the *mNG* reporter gene
413 showed that endogenous and heterologous elements were able to generate fluorescent reporters,
414 albeit with variable efficiency. The pLCh2 vector design containing *tmv* as 3'UTR termination

415 sequence for *psbH* was selected to test different reporter gene conformations due to its capability
416 to generate autonomous *mNG* transcripts, its low homology rate with chloroplast genome
417 sequences in order to diminish unwanted homologous recombination events, and its capability
418 for reporter protein expression as observed in this work.
419
420 Results obtained in this experiment under photoautotrophic conditions showed that the use of
421 heterologous regulatory sequences enabled reporter gene expression, however elements differ in
422 their efficiency compared to endogenous regulatory sequences. As for heterologous terminators,
423 the T*rbcL* (*Nt*Cp) sequence decreased fluorescence levels to half of the control strains using the
424 endogenous T*rbcL* sequence. The T*rbcL* 3'UTR termination sequence forms a hairpin secondary
425 structure, that might act through the RHON1-dependent termination in higher plants, however, it
426 is described to be both gene- and species-specific, which may explain its low performance in *C.*
427 *reinhardtii*'s chloroplast [Chi et al. 2014]. The T*tymv* sequence is known to work mostly as an
428 enhancer for 5' capped mRNAs [Matsuda and Deher, 2005], which is not a common case for
429 chloroplast transcripts [Zhang et al. 2019], which may explain the complete abolishment of
430 fluorescence levels. The use of the *E. coli* T*rrnB* sequence exhibited slightly higher fluorescence
431 levels compared to the control, and had a similar trend as a functional terminator for the psbH
432 selectable gene in this work. This implies that highly divergent prokaryote terminators are
433 functional in chloroplasts of *C. reinhardtii* likely through conserved mechanisms of
434 factor-independent termination [Orosz et al., 1991].
435
436 In the case of heterologous promoters, different sequences were selected from promoters
437 activated exclusively by PEP (P*psbA*), by NEP (P*rpoB*) or by both (P*rbcL*). All heterologous
438 promoters diminished fluorescence levels, however PpsbA (*NtCp)* abolished fluorescence
439 completely, PrcbL (*NtCp)* exhibited a ~0.5 level and PrpoB (*NtCp*) conserved a ~0.38
440 fluorescence level compared to the control. Results obtained in this work agree with the results
441 reported by previous work where heterologous promoters support gene expression in *C.*
442 *reinhardtii*'s chloroplast [Gimpel et al. 2012]. Further, we observed that the use of an
443 heterologous psbA (*NtCp*) 5'UTR enabled fluorescence levels up to half of the control, in
444 contrast what was reported that only heterologous 5'UTR from *C. reinhardtii* could support
445 translation of a D1 protein, likely to secondary structure recognition by endogenous factors

[Gimpel et al. 2012]. While their experiments used heterologous expression of the D1, a photosystem II protein required for photosynthesis and autotrophic growth in minimal media, the fluorescence reporter used in this study is not required for cell viability and thus is likely to be tolerant of a larger range of expression levels.

Related to the endogenous promoters and 5'UTR sequences used in this work, replacing the *atpA* promoter by P*rrnS* increased fluorescence reporter levels to double of the positive control, and this improvement was attenuated in phototrophic conditions when the *atpA* 5'UTR was replaced with the *psbA* 5'UTR. This is in agreement with results obtained in other works, and it is attributed to auto-attenuation of *psbA* 5'UTR dependent from the *psbA* product D1 protein [Rasala et al. 2011].

Chloroplast-encoded fluorescent reporter accumulates mainly in the pyrenoid periphery.

Images obtained by confocal microscopy suggest that expression of fluorescent reporter gene from the *psbH* locus lead to heterogeneous mNG accumulation in the chloroplast stroma without signal depletion of the pyrenoid, which included higher accumulation in the pyrenoid periphery. Other works have described that exclusion of proteins higher than ~50kDa from the pyrenoid matrix may occur [Mackinder et al., 2018], this might be happening with mNG due its effective molecular weight observed at ~70kDa by native-PAGE in this work. Presence of mNG specifically in the pyrenoid periphery could have not been identified through epifluorescence microscopy due to out of focus fluorescence from other optical planes. The use of the chloroplast-encoded *mNG* fluorescent reporter described in this study can aid in gaining deeper understanding of aspects of subcellular and molecular biology in the chloroplast of *C. reinhardtii*.

472 **METHODS**

473

474 **Cell strains, culture conditions and maintenance**

475 The *C. reinhardtii* cell wall deficient strain TN72 cw15 ΔpsbH [Young et al. 2014] was obtained
476 from Chlamydomonas Resource Center's collection (https://www.chlamycollection.org), listed
477 as CC-5168. Handling of cultures was performed according to standard protocols [Harris, 2009].
478 Agar stabs were streaked in 2% agar TAP plates (Phytotech Labs, T8224), re-streaked in 1.2%
479 agar (Winkler, 101150) YTAP (TAP + 0.4% w/w yeast extract) plates. Strains were restreaked
480 every 3-4 weeks. Sueoka's High Salt medium (HSM) (Phytotech Labs, S7668) was used for
481 liquid culture and vacuum-filtered prior to autoclaving. Cultures were grown heterotrophically
482 using > 10 PPFD, and photoautotrophically or mixotrophically using ~50 PPFD, with 3000K
483 LED lighting [Baer et al. 2016]. Growth conditions used were 100 rpm agitation and 25 °C. OD
484 was measured at 750 nm by spectroscopy to calculate growth rates and predict ODs for
485 transformation.

486

487 **Plasmid construction**

488 DNA manipulations were carried out following standard protocols [Green and Sambrook, 2012].
489 The pASapI vector was obtained from Chlamydomonas Resource Center and oligonucleotides
490 were designed (Supplementary Table 1) to create modular DNA parts compatible with the uLoop
491 assembly system [Pollak et al. 2020] through PCR products from the pASapI vector or duplex
492 oligonucleotides obtained from Macrogen Inc. (Seoul, Korea). PCR reactions were conducted
493 using Phusion High-Fidelity DNA Polymerase (Thermo Fisher Scientific, F530S) according to
494 the manufacturer's protocol. Cloning of Level 0 (L0) vectors was performed with PCR products
495 and annealed oligonucleotides purified by isopropanol precipitation [Green and Sambrook,
496 2016], cloned into the pL0R-mRFP1 vector receiver (Figure S5) using Golden-Gate assembly
497 [Engler et al., 2008]. Vectors were verified through Sanger sequencing by Macrogen, or using a
498 Flongle cell (Nanopore, FLO-FLG114) in a MinION device (Oxford Nanopore Technologies,
499 Oxford, UK) and a Rapid Barcoding Kit (Nanopore, SQK-RBK114) according to manufacturer's
500 protocol. L2 transformation vectors were constructed according to uLoop assembly protocol
501 [Pollak et al. 2019, 2020] and different designs were used for arrangement of modules (Figure
502 S1b). Vector containing codon-optimised fluorescent reporter with addition of uLoop-compatible

503 L0 parts was synthesized by Twist Bioscience (South San Francisco, CA, USA).
504 Codon-optimisation was designed using the "most frequent" algorithm used by the CSO software
505 [Weiner et al. 2020], which is based on Kazusa's codon usage table for *C. reinhardtii* chloroplast
506 [Nakamura et al. 2000]. To create negative control strains, the AF-spacer1 (Pollak et al, 2020)
507 was used instead of the reporter gene.
508
509 Chloroplast heterologous regulatory sequences were selected from the MoChlo kit
510 (https://www.addgene.org/kits/lenaghan-mochlo) [Occhialini et al. 2019]. Terminators used for
511 *psbH* were T*psbA* from *Nicotiana tabacum*'s chloroplast (*Nt*Cp), T*tmv* from Tobacco Mosaic
512 Virus, and T*rrnB* from *Escherichia coli* (*Ec*), from the MoChlo kit; and the T*rbcL* sequence from
513 the *C. reinhardtii*'s chloroplast (*Cr*Cp), which was cloned from the pASapI vector. Also, three
514 promoters (P*psbA Nt*Cp, P*rbcL Nt*Cp, P*rpoB Nt*Cp) one 5'UTR (*psbA Nt*Cp 5'UTR), and three
515 3'UTR (T*rbcL*, T*tymv*, T*rrnB Ec*) were selected from the MoChlo kit to assemble promoter,
516 5'UTR and terminator combinations for characterisation of regulatory elements. Endogenous
517 sequences for P*rnnS* and *psbA* 5'UTR were cloned directly from *C. reinhardtii* TN72 strain using
518 listed primers (Supplementary Table 1)
519
520 Due to antibiotic resistance incompatibility between MoChlo and uLoop assembly systems, L1
521 odd receiver vectors with ampicillin (pCAampOdd) or chloramphenicol (pCAchlorOdd)
522 resistance were generated through Gibson assembly [Gibson et al. 2009] using uLoop specific
523 primers (Supplementary Table 1), to be used as shuttle vectors for cloning into L2 vectors.
524 Depending on the pLCh design chosen for chloroplast transformation, assembled L1 vectors
525 were used as donors to assemble the Level 2 (L2) pLCh vectors using the pHCe1 receiver vector,
526 a pCAe-1 (Pollak et al., 2020) with a modification in the pBR322 ORI to enable high-copy
527 number as described for the pUC ORI [Lin-Chao et al., 1992]. pHCe1 vectors were generated by
528 Golden-Gate assembly using AarI enzyme and specified primers (Supplementary Table 1). L2
529 vector designs were based in different arrays of the pASapI vector (Figure S1b), and were used
530 directly for glass-beads chloroplast transformation of *C. reinhardtii*.

531

532 **uLoop assembly, bacterial transformation and plasmid purification**

533 uLoop assembly was performed according to Pollak et al. 2019, 2020,
534 (https://www.protocols.io/view/loop-and-uloop-assembly-yxnfxme), with minor adaptations.
535 DNA was quantified by fluorimetry using the Quantus™ Fluorometer (Promega, E6150) with
536 the QuantiFluor® dsDNA System (Promega, E2670) according to manufacturer's specifications.
537 Concentrations of 5 fmol/µL for donor parts and 2.5 fmol/µL for receiver plasmids were used in
538 assembly reactions. Plasmids were purified using Wizard® Plus SV Minipreps DNA
539 Purification System (Promega, A1470) and validated by restriction digest and sequencing.
540 Plasmid purification from 50 mL bacterial cultures was made using PureYield™ Plasmid
541 Midiprep System (Promega, A2492) for *C. reindhartii*'s chloroplast transformations.

542

543 **Chloroplast transformation and verification of homoplasmicity**

544 Chloroplast transformation was performed using the glass beads chloroplast transformation
545 method (Kindle et al. 1991) with modifications (Economou et al., 2014) for DNA integration
546 into the *psbH* locus by homologous recombination (Figure S3). Exceptions to the protocol were
547 that DNA used for transformation was measured by fluorometry and fixed to be 10 µg (Figure
548 S1a). Liquid cultures were grown in a BJPX-200B refrigerated shaker incubator (Biobase, Jinan,
549 Shandong, China) at 100 RPM at 25 °C, and transformation plates were incubated at 25°C in a
550 JSR refrigerated incubator modified with 3000K warm white LED lights to provide 200 PPFD,
551 avoiding light saturation conditions [Virtanen et al. 2019].

552

553 Transformant colonies were restreaked after 2-3 weeks, 1-2 times on selective media before
554 homoplasmicity was determined. A loopful of cells was used from isolated colonies, resuspended
555 in 180 µL of HSM liquid media and 90 µL were transferred to a new 1.5 mL tube, where total
556 genomic DNA was extracted adding 10 µL of Edwards Extraction Buffer [Kasajima et al. 2004].
557 *C. reinhardtii* cells were homogenized by pipetting softly, and 1 µL was directly used for
558 homoplasmicity confirmation through PCR amplification using a combination of three primers
559 (Supplementary Table 1) for a duplex PCR reaction (Figure S4).

560

561 ***In vivo* microplate fluorometry**

562 Strains were grown under photoautotrophic, mixotrophic or heterotrophic conditions to late-log
563 phase before evaluation. Fluorescence levels were measured by microplate fluorometry using a
564 Synergy H1 Hybrid multimode reader (BioTek Instruments, Vermont, USA). Triplicates of 200
565 uL for each strain cell culture were transferred into Nunc 96-well black/clear bottom plates
566 (Thermo Scientific, 165305). mNeongreen detection was performed using Ex: 505/12 nm and
567 Em: 535/12 nm, with gain set at 120. HSM medium was used for photoautotrophic conditions
568 and TAP medium was used for heterotrophic and mixotrophic conditions. Fluorescence values
569 were normalized on the basis of $OD_{750\ nm}$ in cell cultures. Transplastomic strains with absence of
570 fluorescent reporter were used for background subtraction.

571

572 **Fluorescence microscopy**

573 Liquid cell cultures under different conditions were grown to late-log phase in photoautotrophic
574 conditions for light and epifluorescence microscopy; and under mixotrophic conditions for
575 confocal microscopy. To visualize structures different from the chloroplast, cells were stained
576 with DAPI with the following method: 5 µL of DAPI solution (Invitrogen, D1306; 0.5 mg ml^{-1}
577 dissolved in 250 mM sucrose) were mixed with 15 µL of late-log phase cell culture (1-5 x 10^6
578 cells/mL) and incubated for 5 min in the dark before visualization.

579

580 Epifluorescence microscopy was performed in an Axio Imager.M2 microscope (Zeiss, Jena,
581 Germany) equipped with Colibri 7 LED light for excitation at 475 nm for Chl channel, 511 nm
582 for mNG channel, and 385 nm for DAPI channel, with corresponding filters used for Chl (Ex.
583 480/30 nm, Em. 600 nm longpass), mNG (Ex. 495/20 nm, Em. 540/30 nm) and DAPI (Ex. 365
584 nm, Em. 445/50 nm). Transmitted light was used for wide-field DIC channel. Chloroplast
585 sub-localization of mNeongreen was determined by confocal microscopy in a LSM 880
586 AiryScan microscope (Zeiss, Jena, Germany), using a 633 HeNe laser for excitation of
587 chlorophyll, a multiline argon laser for excitation (at 458/488/514 nm) of fluorescent protein, and
588 a 405 diode laser 30mW for DAPI. Filters were used for Chl channel (Em. 645 nm longpass),
589 mNG channel (Ex. 470/40 nm, Em. 525/50 nm) and DAPI channel (Ex. 365 nm, Em.
590 445/50 nm).

591

592

593 **Transcript analysis by semiquantitative RT-PCR and absolute quantification RT-qPCR.**

594 Liquid cell cultures (10 mL) were grown to late-log phase in photoautotrophic standard
595 conditions for total RNA extractions using the GenElute Total RNA Purification Kit
596 (Sigma-Aldrich, RNB100) by following manufacturer instructions with the following
597 modifications. In the disruption step, cells were homogenized into the disruption buffer only by
598 pipetting, since vortexing drastically decreases RNA yield. Total RNA extracts were treated with
599 Turbo DNAse (Invitrogen, AM2238) for gDNA depletion following manufacturer's instructions.
600 For semiquantitative RT-PCR, cDNA was synthesized from total RNA using M-MLV Reverse
601 Transcriptase (Promega, M1701) using listed primers (Supplementary Table 1). PCR reactions
602 using cDNA as template were performed and PCR products were separated by agarose gel
603 electrophoresis in an 1% w/v agarose gel (Lonza, 50004) using 100V during 30 min. For
604 absolute quantification of transcripts by RT-qPCR, KAPA SYBR FAST One-Step RT-qPCR kit
605 (Roche, KK4650) was used following manufacturer protocols. Amplification of transcript
606 segments from *mNG* and readthrough transcripts using total RNA as template was performed
607 using a CFX96 Touch Real-Time PCR Detection System (Bio-Rad Laboratories, CA, USA)
608 using listed primers (Supplementary Table 1). For calibration curves, products obtained in
609 previous RT-PCR reactions were used as template for the respective transcript quantification.

610

611 **Protein extraction and native polyacrylamide gel electrophoresis.**

612 Total soluble protein extracts were prepared using pelleted algal cells from 10 mL late-log phase
613 photoautotrophic cultures, pellets were resuspended in 300 µl of Breaking buffer pH 7.5,
614 prepared with 50 mM NaH2PO4 (Merck, 106346), 1 mM EDTA (Thermo Scientific, E9884), 5%
615 v/v glycerol (Winkler, BM-0800), 1 mM PMSF (Sigma-Aldrich, P7626). Resuspended cells were
616 transferred to a glass test tube with 300 mg of acid-washed glass beads, followed by disruption
617 of cells by vortex at full speed for 3 cycles that consisted in 1 min vortexing followed by 1 min
618 of ice incubation. Lysates were transferred into Eppendorf tubes for centrifugation at 15000 x g
619 for 5 min at 4°C for removal of cell debris and glass beads. Then, the supernatant was recovered
620 and stored at 4°C. Protein amounts were quantified using Coomassie (Bradford) Protein Assay
621 Kit (Thermo Fisher Scientific, 23200) following manufacturer's instructions. Native
622 polyacrylamide gel electrophoresis (native-PAGE) was performed with standard protocol

[Harlow and Lane 1988]. Resolving gel was prepared at 15% v/v acrylamide, stacking gel at 5% v/v acrylamide, and electrophoresis was performed using 8V/cm during 90 min. Excitation of fluorescent samples in gel was made with a blue light and the yellow filter from the Stereo Microscope Fluorescence system (Nightsea, PA, USA).

Statistical Analyses

Statistical analyses were performed with the Prism 8.0.1 statistical package (GraphPad Software Inc., California, USA). Following confirmation of normality and homogeneity of variance, significant differences between different samples with a single culture condition were determined by one-way ANOVA, two-way ANOVA was used for multiple culture conditions; both included Tukey's multiple comparison post-hoc test, at a 95% confidence interval. For absolute quantification of transcripts, significant differences of transcript levels within the same sample were determined by multiple t-tests, significant differences between different samples were determined by one-way ANOVA, Tukey's multiple comparison post-hoc test with 95% confidence interval.

AUTHOR CONTRIBUTIONS

Axel Navarrete: Investigation, Methodology, Formal Analysis, Visualization, Writing- Original draft preparation. **Bernardo Pollak:** Conceptualization, Methodology, Supervision, Visualization Writing- Review and Editing, Funding acquisition.

ACKNOWLEDGEMENTS

We would like to thank Dr. Diego Lagos and Karina Olivos for providing uLoop vector receivers and their guidance related to assembly methods, Javiera Soto-Aguilar for her guidance in protein electrophoresis methods, Dr. Juan Jimenez for his guidance in RT-qPCR protocols, and Dr. Chloe Economou together with Dr. Harry Jackson for their guidance in the *C. reinhardtii* glass-bead chloroplast transformation method, and kindly providing a vector encoding a bioluminescent reporter gene for *C. reinhardtii* chloroplast expression. We would like to acknowledge Professor Dr. Rodrigo Gutierrez for reading the manuscript and providing useful comments and advice, Dr. Stephanie Braun-Galleani and Dr. Javier Gimpel for comments regarding the findings, Professor Dr. Luis Larrondo for general guidance, and Dr. Susana Cabello for help with project administration.

This work was financed by FONDECYT Iniciación 11190303 to B.P. through the Instituto Milenio de Biología Integrativa (iBio). B.P. was provided support from Fundación Ciencia y Vida through the Programa de Apoyo a Centros con Financiamiento Basal AFB 170004.

REFERENCES

[1] Boynton, J. E., Gillham, N. W., Harris, E. H., Hosler, J. P., Johnson, A. M., Jones, A. R., ... & Sanford, J. C. (1988). Chloroplast transformation in Chlamydomonas with high velocity microprojectiles. Science, 240(4858), 1534-1538. https://doi.org/10.1126/science.2897716

[2] Svab, Z., Hajdukiewicz, P., & Maliga, P. (1990). Stable transformation of plastids in higher plants. Proceedings of the National Academy of Sciences, 87(21), 8526-8530. https://doi.org/10.1073/pnas.87.21.8526

[3] Kindle, K. L., Richards, K. L., & Stern, D. B. (1991). Engineering the chloroplast genome: techniques and capabilities for chloroplast transformation in Chlamydomonas reinhardtii. Proceedings of the National Academy of Sciences, 88(5), 1721-1725. https://doi.org/10.1073/pnas.88.5.1721

[4] Young, R. E., & Purton, S. (2014). Cytosine deaminase as a negative selectable marker for the microalgal chloroplast: a strategy for the isolation of nuclear mutations that affect chloroplast gene expression. The Plant Journal, 80(5), 915-925. https://doi.org/10.1111/tpj.12675

[5] Wannathong, T., Waterhouse, J. C., Young, R. E., Economou, C. K., & Purton, S. (2016). New tools for chloroplast genetic engineering allow the synthesis of human growth hormone in the green alga Chlamydomonas reinhardtii. Applied microbiology and biotechnology, 100, 5467-5477. https://doi.org/10.1007/s00253-016-7354-6

[6] Franklin, S., Ngo, B., Efuet, E., & Mayfield, S. P. (2002). Development of a GFP reporter gene for Chlamydomonas reinhardtii chloroplast. The Plant Journal, 30(6), 733-744. https://doi.org/10.1046/j.1365-313X.2002.01319.x

[7] Braun−Galleani, S., Baganz, F., & Purton, S. (2015). Improving recombinant protein production in the Chlamydomonas reinhardtii chloroplast using vivid Verde Fluorescent Protein as a reporter. Biotechnology journal, 10(8), 1289-1297.
https://doi.org/10.1002/biot.201400566

[8] Karcher, D., Köster, D., Schadach, A., Klevesath, A., & Bock, R. (2009). The Chlamydomonas chloroplast HLP protein is required for nucleoid organization and genome maintenance. Molecular plant, 2(6), 1223-1232.
https://doi.org/10.1093/mp/ssp083

[9] Lauersen, K. J., Kruse, O., & Mussgnug, J. H. (2015). Targeted expression of nuclear transgenes in Chlamydomonas reinhardtii with a versatile, modular vector toolkit. Applied microbiology and biotechnology, 99, 3491-3503.
https://doi.org/10.1007/s00253-014-6354-7

[10] Crozet, P., Navarro, F.J., Willmund, F., Mehrshahi, P., Bakowski, K., Lauersen, K.J., Pérez-Pérez, M.E., Auroy, P., Gorchs Rovira, A., Sauret-Gueto, S., & Niemeyer, J. (2018). Birth of a photosynthetic chassis: a MoClo toolkit enabling synthetic biology in the microalga Chlamydomonas reinhardtii. ACS synthetic biology, 7(9), 2074-2086.
https://doi.org/10.1021/acssynbio.8b00251

[11] Stern, D. B., Goldschmidt-Clermont, M., & Hanson, M. R. (2010). Chloroplast RNA metabolism. Annual review of plant biology, 61, 125-155.
https://doi.org/10.1146/annurev-arplant-042809-112242

[12] Barkan, A. (2011). Expression of plastid genes: organelle-specific elaborations on a prokaryotic scaffold. Plant physiology, 155(4), 1520-1532.
https://doi.org/10.1104/pp.110.171231

[13] Ji, D., Manavski, N., Meurer, J., Zhang, L., & Chi, W. (2019). Regulated chloroplast transcription termination. In Biochimica et Biophysica Acta (BBA) - Bioenergetics (Vol. 1860, Issue 1, pp. 69–77). Elsevier BV.
https://doi.org/10.1016/j.bbabio.2018.11.011

[14] Shi, C., Wang, S., Xia, E. H., Jiang, J. J., Zeng, F. C., & Gao, L. Z. (2016). Full transcription of the chloroplast genome in photosynthetic eukaryotes. Scientific reports, 6(1), 30135.
https://doi.org/10.1038/srep30135

[15] Rott, R., Schuster, G., Drager, R. G., & Stern, D. B. (1996). The 3′ untranslated regions of chloroplast genes in Chlamydomonas reinhardtii do not serve as efficient transcriptional terminators. Molecular and General Genetics MGG, 252, 676-683.
https://doi.org/10.1111/pbi.13985

[16] Young, R. E., & Purton, S. (2016). Codon reassignment to facilitate genetic engineering and biocontainment in the chloroplast of Chlamydomonas reinhardtii. Plant biotechnology journal, 14(5), 1251-1260.
https://doi.org/10.1111/pbi.12490

[17] Kim, S. Y., Kim, K. W., Kwon, Y. M., & Kim, J. Y. H. (2020). mCherry protein as an in vivo quantitative reporter of gene expression in the chloroplast of Chlamydomonas reinhardtii. Molecular Biotechnology, 62(5), 297-305.
https://doi.org/10.1007/s12033-020-00249-9

[18] Bertalan, I., Munder, M. C., Weiß, C., Kopf, J., Fischer, D., & Johanningmeier, U. (2015). A rapid, modular and marker-free chloroplast expression system for the green alga Chlamydomonas reinhardtii. Journal of biotechnology, 195, 60-66.
https://doi.org/10.1016/j.jbiotec.2014.12.017

[19] Patron, N. J., Orzaez, D., Marillonnet, S., Warzecha, H., Matthewman, C., Youles, M., ... & Haseloff, J. (2015). Standards for plant synthetic biology: a common syntax for exchange of DNA parts. New Phytologist, 208(1), 13-19.
https://doi.org/10.1111/nph.13532

[20] Occhialini, A., Piatek, A. A., Pfotenhauer, A. C., Frazier, T. P., Stewart Jr, C. N., & Lenaghan, S. C. (2019). MoChlo: a versatile, modular cloning toolbox for chloroplast biotechnology. Plant physiology, 179(3), 943-957.
https://doi.org/10.1104/pp.18.01220

[21] Pollak, B., Matute, T., Nuñez, I., Cerda, A., Lopez, C., Vargas, V., Kan, A., Bielinski, V., von Dassow, P., Dupont, C., & Federici, F. (2020). "Universal loop assembly: open, efficient and cross-kingdom DNA fabrication, Synthetic Biology 5 (1).
https://doi.org/10.1093/synbio/ysaa001

[22] Taparia, Y., Dolui, A. K., Boussiba, S., & Khozin-Goldberg, I. (2022). Multiplexed Genome Editing via an RNA Polymerase II Promoter-Driven sgRNA Array in the Diatom Phaeodactylum tricornutum: Insights Into the Role of StLDP. Frontiers in Plant Science, 12, 3053.
https://doi.org/10.3389/fpls.2021.784780

[23] Moosburner, M., Allen, A. E., & Daboussi, F. (2022). Genetic Engineering in Marine Diatoms: Current Practices and Emerging Technologies. The Molecular Life of Diatoms, 743-773.
https://doi.org/10.1007/978-3-030-92499-7_25

[24] Arce, A., Guzman Chavez, F., Gandini, C., Puig, J., Matute, T., Haseloff, J., Dalchau, N., Molloy, J., Pardee, K. & Federici, F. (2021). Decentralizing cell-free RNA sensing with the use of low-cost cell extracts. Frontiers in Bioengineering and Biotechnology, 9, 727584.
https://doi.org/10.3389/fbioe.2021.727584

[25] Ishikura, K., Takaoka, Y., Kato, K., Sekine, M., Yoshida, K., & Shinmyo, A. (1999). Expression of a foreign gene in Chlamydomonas reinhardtii chloroplast. Journal of Bioscience and Bioengineering, 87(3), 307-314.
https://doi.org/10.1016/S1389-1723(99)80037-1

[26] Gallaher, S. D., Fitz−Gibbon, S. T., Strenkert, D., Purvine, S. O., Pellegrini, M., & Merchant, S. S. (2018). High−throughput sequencing of the chloroplast and mitochondrion of Chlamydomonas reinhardtii to generate improved de novo assemblies, analyze expression patterns and transcript speciation, and evaluate diversity among laboratory strains and wild isolates. The Plant Journal, 93(3), 545-565.
https://doi.org/10.1111/tpj.13788

[27] Jackson, H. O., Taunt, H. N., Mordaka, P. M., Kumari, S., Smith, A. G., & Purton, S. (2022). CpPosNeg: A positive−negative selection strategy allowing multiple cycles of marker−free engineering of the Chlamydomonas plastome. Biotechnology Journal, 17(10), 2200088.
https://doi.org/10.1002/biot.202200088

[28] Rasala, B.A., Barrera, D.J., Ng, J., Plucinak, T.M., Rosenberg, J.N., Weeks, D.P., Oyler, G.A., Peterson, T.C., Haerizadeh, F. and Mayfield, S.P. (2013). Expanding the spectral palette of fluorescent proteins for the green microalga Chlamydomonas reinhardtii. The Plant Journal, 74(4), 545-556.
https://doi.org/10.1111/tpj.12165

[29] Noor−Mohammadi, S., Pourmir, A., & Johannes, T. W. (2012). Method to assemble and integrate biochemical pathways into the chloroplast genome of Chlamydomonas reinhardtii. Biotechnology and Bioengineering, 109(11), 2896-2903.
https://doi.org/10.1002/bit.24569

[30] Fields, F. J., Ostrand, J. T., Tran, M., & Mayfield, S. P. (2019). Nuclear genome shuffling significantly increases production of chloroplast-based recombinant protein in Chlamydomonas reinhardtii. Algal Research, 41, 101523.
https://doi.org/10.1016/j.algal.2019.101523

[31] Shaner, N.C., Lambert, G.G., Chammas, A., Ni, Y., Cranfill, P.J., Baird, M.A., Sell, B.R., Allen, J.R., Day, R.N., Israelsson, M. and Davidson, M.W., 2013. A bright monomeric green fluorescent protein derived from Branchiostoma lanceolatum. Nature methods, 10(5), 407-409.
https://doi.org/10.1038/nmeth.2413

[32] Tangphatsornruang, S., Birch-Machin, I., Newell, C. A., & Gray, J. C. (2011). The effect of different 3′ untranslated regions on the accumulation and stability of transcripts of a gfp transgene in chloroplasts of transplastomic tobacco. Plant molecular biology, 76, 385-396.
https://doi.org/10.1007/s11103-010-9689-1

[33] Schein, A., Sheffy-Levin, S., Glaser, F., & Schuster, G. (2008). The RNase E/G-type endoribonuclease of higher plants is located in the chloroplast and cleaves RNA similarly to the E. coli enzyme. Rna, 14(6), 1057-1068.
https://doi.org/10.1261/rna.907608

[34] Kishine, M., Takabayashi, A., Munekage, Y., Shikanai, T., Endo, T., & Sato, F. (2004). Ribosomal RNA processing and an RNase R family member in chloroplasts of Arabidopsis. Plant molecular biology, 55, 595-606.
https://doi.org/10.1007/s11103-004-1507-1

[35] Sharwood, R. E., Halpert, M., Luro, S., Schuster, G., & Stern, D. B. (2011). Chloroplast RNase J compensates for inefficient transcription termination by removal of antisense RNA. Rna, 17(12), 2165-2176.
https://doi.org/10.1261/rna.028043.111

[36] Liponska, A., Jamalli, A., Kuras, R., Suay, L., Garbe, E., Wollman, F.A., Laalami, S., & Putzer, H. (2018). Tracking the elusive 5′ exonuclease activity of Chlamydomonas reinhardtii RNase J. Plant molecular biology, 96, 641-653.
https://doi.org/10.1007/s11103-018-0720-2

[37] De La Sierra-Gallay, I. L., Zig, L., Jamalli, A., & Putzer, H. (2008). Structural insights into the dual activity of RNase J. Nature structural & molecular biology, 15(2), 206-212.
https://doi.org/10.1038/nsmb.1376

[38] Waters, L. S., & Storz, G. (2009). Regulatory RNAs in bacteria. Cell, 136(4), 615-628.
https://doi.org/10.1016/j.cell.2009.01.043

[39] Rochaix, J. D., Kuchka, M., Mayfield, S., Schirmer−Rahire, M., Girard−Bascou, J., & Bennoun, P. (1989). Nuclear and chloroplast mutations affect the synthesis or stability of the chloroplast psbC gene product in Chlamydomonas reinhardtii. The EMBO Journal, 8(4), 1013-1021.
https://doi.org/10.1002/j.1460-2075.1989.tb03468.x

[40] Prikryl, J., Rojas, M., Schuster, G., & Barkan, A. (2011). Mechanism of RNA stabilization and translational activation by a pentatricopeptide repeat protein. Proceedings of the National Academy of Sciences, 108(1), 415-420.
https://doi.org/10.1073/pnas.1012076108

[41] Rott, R., Schuster, G., Drager, R. G., & Stern, D. B. (1996). The 3′ untranslated regions of chloroplast genes in Chlamydomonas reinhardtii do not serve as efficient transcriptional terminators. Molecular and General Genetics MGG, 252, 676-683.
https://doi.org/10.1007/BF02173973

[42] Larrea-Alvarez, M., & Purton, S. (2020). Multigenic engineering of the chloroplast genome in the green alga Chlamydomonas reinhardtii. Microbiology, 166(6), 510.
https://doi.org/10.1099/mic.0.000910

[43] Katz, Y. S., & Danon, A. (2002). The 3′-untranslated region of chloroplast psbA mRNA stabilizes binding of regulatory proteins to the leader of the message. Journal of Biological Chemistry, 277(21), 18665-18669.
https://doi.org/10.1074/jbc.M201033200

[44] Stern, D. B., & Gruissem, W. (1987). Control of plastid gene expression: 3′ inverted repeats act as mRNA processing and stabilizing elements, but do not terminate transcription. Cell, 51(6), 1145-1157.
https://doi.org/10.1016/0092-8674(87)90600-3

[45] Manavski, N., Schmid, L. M., & Meurer, J. (2018). RNA-stabilization factors in chloroplasts of vascular plants. Essays in biochemistry, 62(1), 51-64.
https://doi.org/10.1042/EBC20170061

[46] Van Belkum, A., Abrahams, J. P., Pleij, C. W., & Bosch, L. (1985). Five pseudoknots are present at the 204 nucleotides long 3'noncoding region of tobacco mosaic virus RNA. Nucleic Acids Research, 13(21), 7673.
https://doi.org/10.1093/nar/13.21.7673

[47] Osman, T. A. M., Hemenway, C. L., & Buck, K. W. (2000). Role of the 3′ tRNA-like structure in tobacco mosaic virus minus-strand RNA synthesis by the viral RNA-dependent RNA polymerase in vitro. Journal of virology, 74(24), 11671-11680.
https://doi.org/10.1128/jvi.74.24.11671-11680.2000

[48] Brosius, J., Ullrich, A., Raker, M. A., Gray, A., Dull, T. J., Gutell, R. R., & Noller, H. F. (1981). Construction and fine mapping of recombinant plasmids containing the rrnB ribosomal RNA operon of E. coli. Plasmid, 6(1), 112-118.
https://doi.org/10.1016/0147-619X(81)90058-5

[49] Orosz, A., Boros, I., & Venetianer, P. (1991). Analysis of the complex transcription termination region of the Escherichia coli rrn B gene. European Journal of Biochemistry, 201(3), 653-659.
https://doi.org/10.1111/j.1432-1033.1991.tb16326.x

[50] Eberhard, S., Drapier, D., & Wollman, F. A. (2002). Searching limiting steps in the expression of chloroplast−encoded proteins: relations between gene copy number, transcription, transcript abundance and translation rate in the chloroplast of Chlamydomonas reinhardtii. The Plant Journal, 31(2), 149-160.
https://doi.org/10.1046/j.1365-313X.2002.01340.x

[51] Rasala, B. A., Muto, M., Sullivan, J., & Mayfield, S. P. (2011). Improved heterologous protein expression in the chloroplast of Chlamydomonas reinhardtii through promoter and 5′ untranslated region optimization. Plant biotechnology journal, 9(6), 674-683.
https://doi.org/10.1111/j.1467-7652.2011.00620.x

[52] Chi, W., He, B., Manavski, N., Mao, J., Ji, D., Lu, C., ... & Zhang, L. (2014). RHON1 mediates a Rho-like activity for transcription termination in plastids of Arabidopsis thaliana. The Plant Cell, 26(12), 4918-4932.
https://doi.org/10.1105/tpc.114.132118

[53] Matsuda, D., & Dreher, T. W. (2004). The tRNA-like structure of Turnip yellow mosaic virus RNA is a 3′-translational enhancer. Virology, 321(1), 36-46.
https://doi.org/10.1016/j.virol.2003.10.023

[54] Zhang, H., Zhong, H., Zhang, S., Shao, X., Ni, M., Cai, Z., ... & Xia, Y. (2019). NAD tagSeq reveals that NAD+-capped RNAs are mostly produced from a large number of protein-coding genes in Arabidopsis. Proceedings of the National Academy of Sciences, 116(24), 12072-12077.
https://doi.org/10.1073/pnas.1903683116

[55] Gimpel, J. A., & Mayfield, S. P. (2013). Analysis of heterologous regulatory and coding regions in algal chloroplasts. Applied microbiology and biotechnology, 97, 4499-4510. https://doi.org/10.1007/s00253-012-4580-4

[56] Mackinder, L.C., Chen, C., Leib, R.D., Patena, W., Blum, S.R., Rodman, M., Ramundo, S., Adams, C.M. & Jonikas, M.C. (2017). A spatial interactome reveals the protein organization of the algal CO2-concentrating mechanism. Cell, 171(1), 133-147. https://doi.org/10.1016/j.cell.2017.08.044

[57] Harris, E.H. (1989). Culture and storage methods. The Chlamydomonas Sourcebook. A Comprehensive Guide to Biology and Laboratory Use,.25-63. https://doi.org/10.1016/B978-0-12-326880-8.50007-9

[58] Baer, S., Heining, M., Schwerna, P., Buchholz, R., & Hübner, H. (2016). Optimization of spectral light quality for growth and product formation in different microalgae using a continuous photobioreactor. Algal research, 14, 109-115. https://doi.org/10.1016/j.algal.2016.01.011

[59] Green, M. R., & Sambrook, J. (2021). Cloning and transformation with plasmid vectors. Cold Spring Harbor Protocols, 2021(11), pdb-top101170 https://doi.org/10.1101/pdb.top101170

[60] Green, M. R., & Sambrook, J. (2017). Precipitation of DNA with Isopropanol. Cold Spring Harbor Protocols, 2017(8), pdb-prot093385. https://doi.org/10.1101/pdb.prot093385

[61] Engler, C., Kandzia, R., & Marillonnet, S. (2008). A one pot, one step, precision cloning method with high throughput capability. PloS one, 3(11), e3647. https://doi.org/10.1371/journal.pone.0003647

[62] Weiner, I., Feldman, Y., Shahar, N., Yacoby, I., & Tuller, T. (2020). CSO–A sequence optimization software for engineering chloroplast expression in Chlamydomonas reinhardtii. Algal Research, 46, 101788.
https://doi.org/10.1016/j.algal.2019.101788

[63] Nakamura, Y., Gojobori, T., & Ikemura, T. (2000). Codon usage tabulated from international DNA sequence databases: status for the year 2000. Nucleic acids research, 28(1), 292-292.
https://doi.org/10.1093/nar/28.1.292

[64] Gibson, D. G., Young, L., Chuang, R. Y., Venter, J. C., Hutchison III, C. A., & Smith, H. O. (2009). Enzymatic assembly of DNA molecules up to several hundred kilobases. Nature methods, 6(5), 343-345.
https://doi.org/10.1038/nmeth.1318

[65] Lin−Chao, S., Chen, W. T., & Wong, T. T. (1992). High copy number of the pUC plasmid results from a Rom/Rop−suppressible point mutation in RNA II. Molecular microbiology, 6(22), 3385-3393.
https://doi.org/10.1111/j.1365-2958.1992.tb02206.x

[66] Economou, C., Wannathong, T., Szaub, J., & Purton, S. (2014). A simple, low-cost method for chloroplast transformation of the green alga Chlamydomonas reinhardtii. Chloroplast biotechnology: Methods and protocols, 401-411.
https://doi.org/10.1007/978-1-62703-995-6_27

[67] Virtanen, O., Valev, D., Kruse, O., Wobbe, L., & Tyystjarvi, E. (2019). Photoinhibition and continuous growth of the wild-type and a high-light tolerant strain of Chlamydomonas reinhardtii. Photosynthetica, 57(2), 617-626.
https://doi.org/10.32615/ps.2019.056

[68] Kasajima, I., Ide, Y., Ohkama-Ohtsu, N., Hayashi, H., Yoneyama, T., & Fujiwara, T. (2004). A protocol for rapid DNA extraction from Arabidopsis thaliana for PCR analysis. Plant Molecular Biology Reporter, 22, 49-52.
https://doi.org/10.1007/BF02773348

[69] Harlow, E. D., & Lane, D. (1988). A laboratory manual. New York: Cold Spring Harbor Laboratory, 579, 44.

[70] Ghandour, R., Gao, Y., Laskowski, J., Barahimipour, R., Ruf, S., Bock, R., & Zoschke, R. (2023). Transgene insertion into the plastid genome alters expression of adjacent native chloroplast genes at the transcriptional and translational levels. Plant Biotechnology Journal, 21(4), 711-725.
https://doi.org/10.1111/pbi.13985

1002 **FIGURE LEGENDS**

1003

1004 **Figure 1**

1005 *In vivo* fluorescence levels of *C. reinhardtii* transplastomic strains using different
1006 uLoop-assembled vectors containing fluorescent green reporter mNeonGreen (mNG).

1007

1008 **a)** Fluorescent protein localization in different transplastomic strains determined by
1009 epifluorescence microscopy. Insertion unit configurations of the *psbH* locus of each strain are
1010 shown in the left. Images show transmitted light (DIC) and fluorescent channels, where
1011 chlorophyll autofluorescence (Chl) is represented in red, mNeonGreen fluorescence (mNG) in
1012 green, and DAPI staining in blue, respectively. A merged image of all fluorescent channels
1013 (F-Merged) was added. Images shown were taken under the same conditions, are unprocessed
1014 and were chosen as representatives from 10 different images taken for each strain.

1015

1016 **b)** Relative fluorescence units (RFU) normalized by optical density at 750 nm (OD750) obtained
1017 by microplate fluorometry. Error bars represent standard error of mean (SE). (experimental
1018 replicates [n_e] = 3, biological replicates [n_b] = 3, technical replicates [n_t] = 3).

1019 **Figure 2**

1020 Context effect modulation of mNeonGreen expression by replacement of the 3'UTR terminator
1021 of the *psbH* selectable gene in *C. reinhardtii* LCh2 transplastomic strains.

1022

1023 **a)** Diagram of the insertion unit of LCh2 strains in the psbH locus. The terminator replaced for
1024 modulating transcriptional readthrough of the psbH selectable gene is depicted in red.

1025

1026 **b)** Number of colonies obtained from glass-bead chloroplast transformation using different
1027 pLCh2 vectors with psbH terminator variants. Transformant colonies were counted in different
1028 weeks after the transformation event. Error bars represent standard error of mean (SE).
1029 (experimental replicates [n_e] = 3, biological replicates [n_b] = 1, technical replicates [n_t] = 3).

1030

1031 **c)** Heatmap of relative fluorescence units (RFU) normalized by optical density at 750 nm
1032 (OD750) obtained by microplate fluorometry of *in vivo* samples of *C. reinhardtii* cultured in
1033 photoautotrophic (HSM), mixotrophic (TAP-L) and heterotrophic (TAP-D) conditions. Values
1034 are relativized to LCh2-*mNG* strains cultured in photoautotrophic conditions (experimental
1035 replicates [n_e] = 3, biological replicates [n_b] = 3, technical replicates [n_t] = 3).

1036

1037 **d)** Fluorescent protein localization in different transplastomic strains determined by
1038 epifluorescence microscopy. Images show transmitted light (DIC) and fluorescent channels,
1039 where chlorophyll autofluorescence (Chl) is represented in red, mNeonGreen fluorescence
1040 (mNG) in green, and DAPI staining in blue, respectively. A merged image of all fluorescent
1041 channels (F-Merged) was added. Images shown were taken under the same conditions, are
1042 unprocessed and were chosen as representatives from 10 different images taken for each strain.

1043

1044 **Figure 3**

1045 Determination of transcriptional readthrough of the *psbH* selection marker gene and
1046 mNeonGreen reporter gene in *C. reinhardtii* transplastomic strains, and their effect in reporter
1047 protein expression.

1048

1049 **a)** Diagram of the RT-PCR experiment strategy for cDNA synthesis from *psbH* mRNA, *mNG*
1050 mRNA, and their readthrough transcripts in LCh1 and LCh2 strains. Position of primer
1051 alignments for cDNA synthesis by reverse transcription of mRNA are depicted with small
1052 directional arrows aligned in transcript, and the primer used is described with its list number in
1053 black next to the PCR product size (Supplementary Table 1). For PCR of LCh1 and LCh2
1054 samples from cDNA, the forward primers used are depicted with its list number in red, and the
1055 reverse primer used was the same used for cDNA synthesis.

1056

1057 **b)** Detection of *psbH* mRNA and its transcriptional readthrough by semiquantitative RT-PCR in
1058 total RNA samples of representative transplastomic strains of *C. reinhardtii*. Amplicons were
1059 separated by agarose gel electrophoresis. PCR products were obtained using cDNA as templates.
1060 Ladders used were 1 kb DNA ladder (NEB, N3232) and GeneRuler 100 bp DNA ladder (Thermo
1061 Scientific, SM0243).

1062

1063 **c)** Detection of *mNG* mRNA and its transcriptional readthrough by semiquantitative RT-PCR in
1064 total RNA samples of representative transplastomic strains of *C. reinhardtii*. Amplicons were
1065 separated by agarose gel electrophoresis. PCR products were obtained using cDNA as templates.
1066 Ladder used was 1 kb Plus DNA ladder (NEB, N3200).

1067

1068 **d)** Determination of proportion of autonomous *mNG* transcripts and *psbH-mNG* transcripts in
1069 relation to total *mNG* transcripts through absolute quantification of transcripts by RT-qPCR.
1070 Graph bars are tagged with the number of copies of total *mNG* transcripts per nanogram of total
1071 RNA of each strain. Error bars represent standard error of mean (SE). (experimental replicates
1072 $[n_e] = 3$, biological replicates $[n_b] = 1$, technical replicates $[n_t] = 3$).

1073

1074 **e)** Detection of mNG protein in total protein extracts of representative transplastomic strains of
1075 *C. reinhardtii* by native polyacrylamide gel electrophoresis. Approximately 10 ug of total protein
1076 were loaded in each well. Bottom picture shows the gel under blue light with a yellow filter.
1077 Upper picture shows the gel after Coomassie Blue staining. Ladder used was PageRuler
1078 Prestained Protein Ladder (10-170kDa) (Thermo Scientific, SM0671).

1079 **Figure 4**

1080 Effect of different combinations of *cis* regulatory elements in fluorescence levels of the reporter
1081 protein mNeonGreen measured in *C. reinhardtii* transplastomic strains obtained using pLCh2
1082 vectors containing P*psbH*-*psbH*-T*tmv* as selectable gene.

1083

1084 **a)** Diagram of the insertion unit of LCh2 strains in psbH locus. Regulatory elements for
1085 characterisation of regulatory elements affecting expression of the gene of interest are depicted in
1086 red.

1087

1088 **b)** Heatmap of relative fluorescence units (RFU) normalized by optical density at 750 nm
1089 (OD750) obtained by microplate fluorometry of *in vivo* samples of *C. reinhardtii* cultured in
1090 photoautotrophic (HSM), mixotrophic (TAP-L) and heterotrophic (TAP-D) conditions. Values
1091 are normalized to the LCh2-A strains cultured in photoautotrophic conditions. Detail of gene of
1092 interest transcriptional unit for each strain is specified on the left. (experimental replicates [n_e] =
1093 3, biological replicates [n_b] = 3, technical replicates [n_t] = 3).

1094 **Figure 5**

1095 Subcellular localization of fluorescent reporter protein and ultrastructure imaging of *C.*
1096 *reinhardtii* chloroplast.

1097

1098 **a)** Progression of the XY plane through 8 different z-axis positions of a LCh2-*mNG* strain.
1099 Images show fluorescent channels, where chlorophyll autofluorescence (Chl) is represented in
1100 red, and mNeonGreen fluorescence (mNG) in green, respectively. A merged image of both
1101 fluorescent channels (F-Merge) was added. Images shown were taken under the same conditions,
1102 and different channels were post-processed to clearly depict fluorescence signals. Z-stack
1103 progression was chosen as representative from 5 different progression experiments done for each
1104 strain.

1105

1106 **b)** Orthogonal plane reconstruction of a LCh2-*mNG* strain. Images shown are merged pictures of
1107 fluorescent channels, where chlorophyll autofluorescence (Chl) is represented in red,
1108 mNeonGreen fluorescence (mNG) in green, and DAPI staining in blue, respectively. Crossline
1109 was placed pointing at the pyrenoid periphery. Images shown were taken under the same
1110 conditions, and different channels were post-processed using the same settings to clearly depict
1111 fluorescence signals. Reconstruction was chosen as representative from 5 different cells imaged
1112 for each strain.

FIGURES AND TABLES

Figure 1

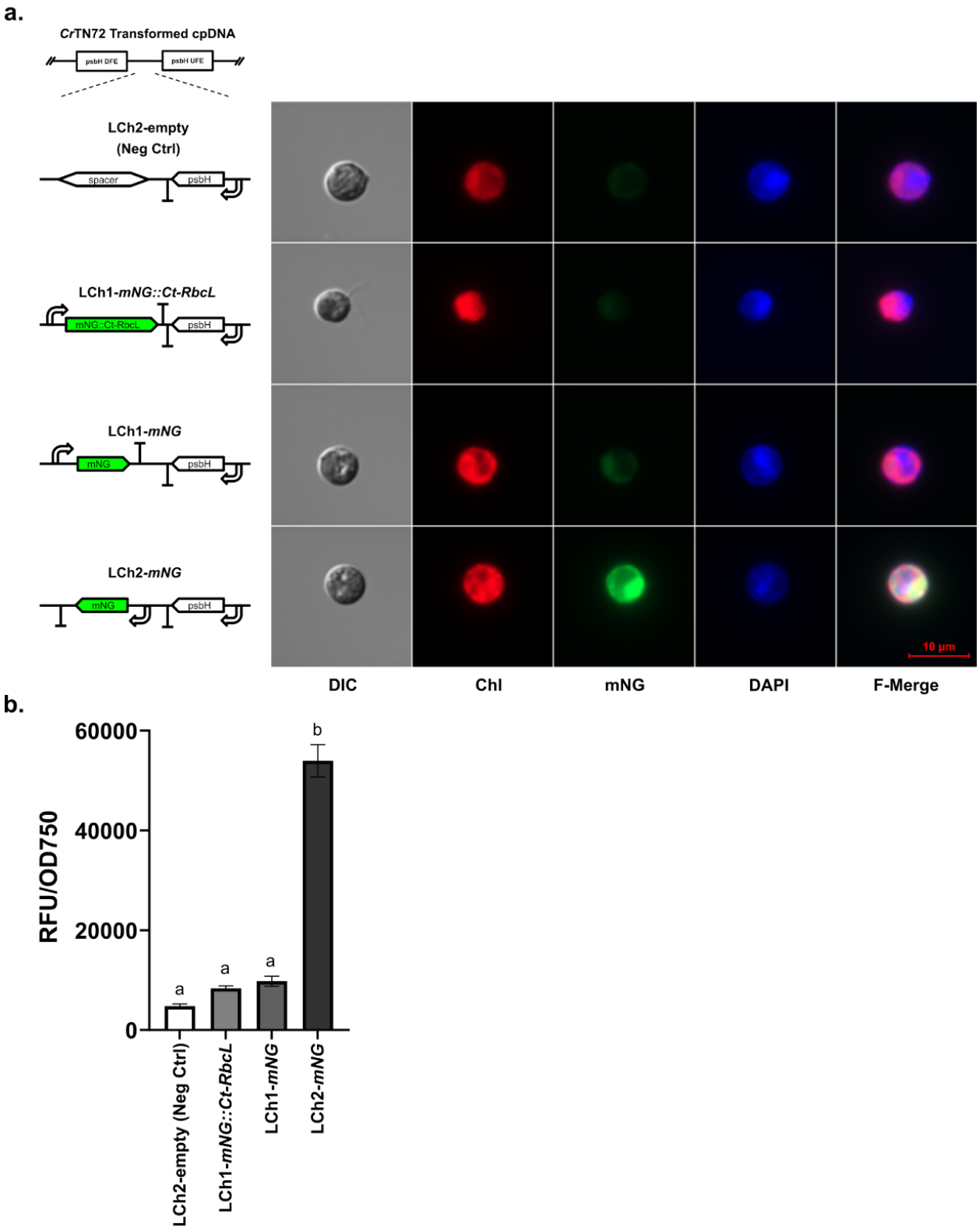

1116 **Figure 2**

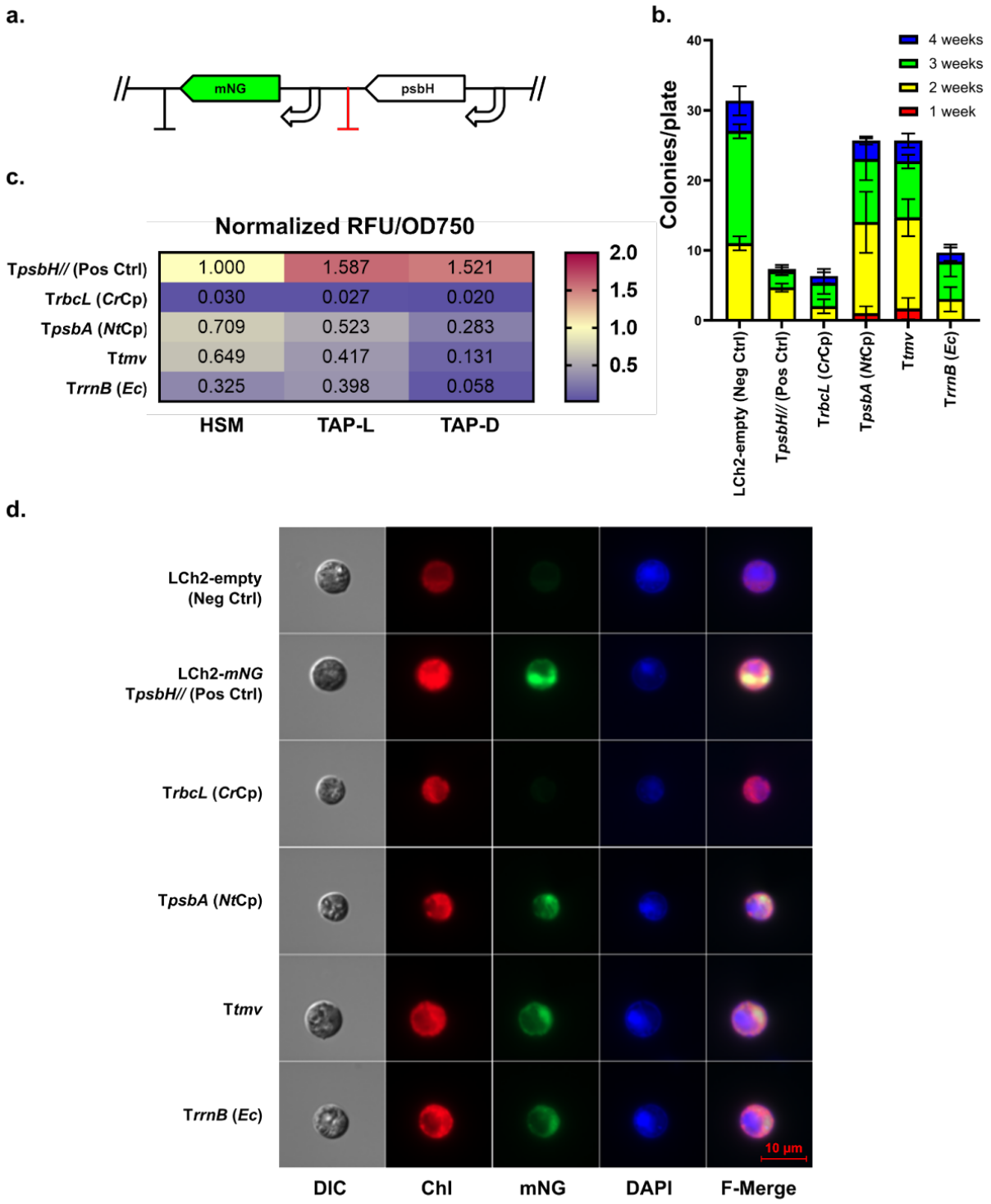

1117

1118 **Figure 3**

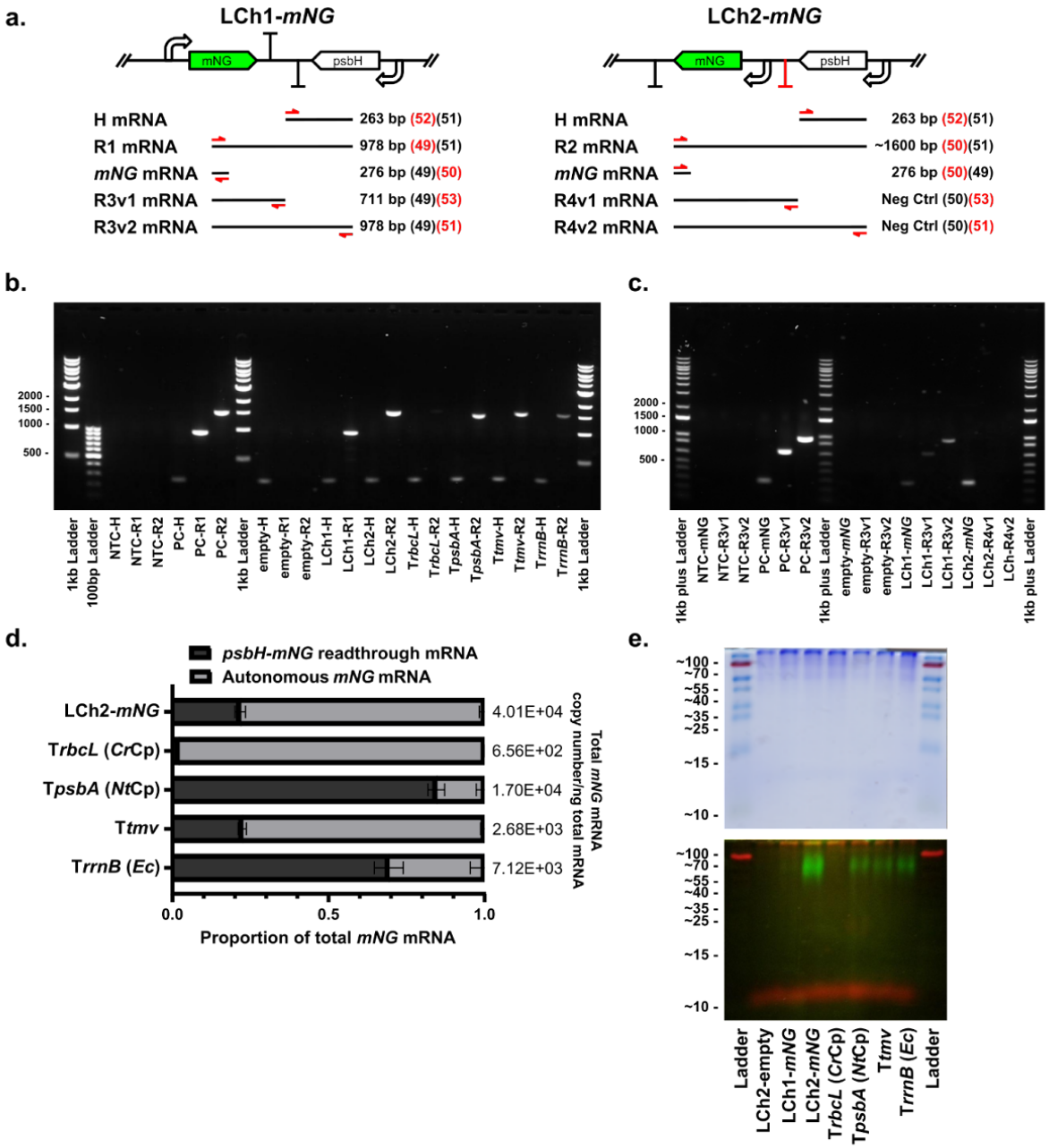

1119

1120 **Figure 4**

a.

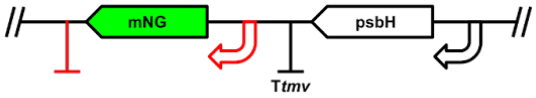

b.

Construct	Promoters	5'UTRs	3'UTRs + Terminators	Normalized RFU/OD750		
				HSM	TAP-L	TAP-D
pLCh2-A (Ctrl)	*atpA* (*Cr*Cp)	*atpA* (*Cr*Cp)	*rbcL* (*Cr*Cp)	1.00	0.73	0.29
pLCh2-B	*atpA* (*Cr*Cp)	*atpA* (*Cr*Cp)	*rbcL* (*Nt*Cp)	0.52	0.17	0.09
pLCh2-C	*atpA* (*Cr*Cp)	*atpA* (*Cr*Cp)	*tymv*	0.12	0.15	0
pLCh2-D	*atpA* (*Cr*Cp)	*atpA* (*Cr*Cp)	*rrnB* (*Ec*)	1.04	0.78	0.33
pLCh2-E	*rrnS* (*Cr*Cp)	*atpA* (*Cr*Cp)	*rbcL* (*Cr*Cp)	2.04	1.41	0.22
pLCh2-F	*rrnS* (*Cr*Cp)	*psbA* (*Cr*Cp)	*rbcL* (*Cr*Cp)	1.09	1.46	0.10
pLCh2-G	*rrnS* (*Cr*Cp)	*psbA* (*Nt*Cp)	*rbcL* (*Cr*Cp)	0.67	0.07	0
pLCh2-H	*psbA* (*Nt*Cp)	*psbA* (*Cr*Cp)	*rbcL* (*Cr*Cp)	0	0.09	0.14
pLCh2-I	*rbcL* (*Nt*Cp)	*psbA* (*Cr*Cp)	*rbcL* (*Cr*Cp)	0.50	0.16	0.30
pLCh2-J	*rpoB* (*Nt*Cp)	*psbA* (*Cr*Cp)	*rbcL* (*Cr*Cp)	0.38	0.47	0.29

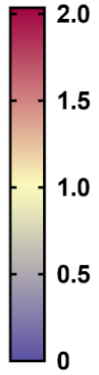

1121

1122 **Figure 5**

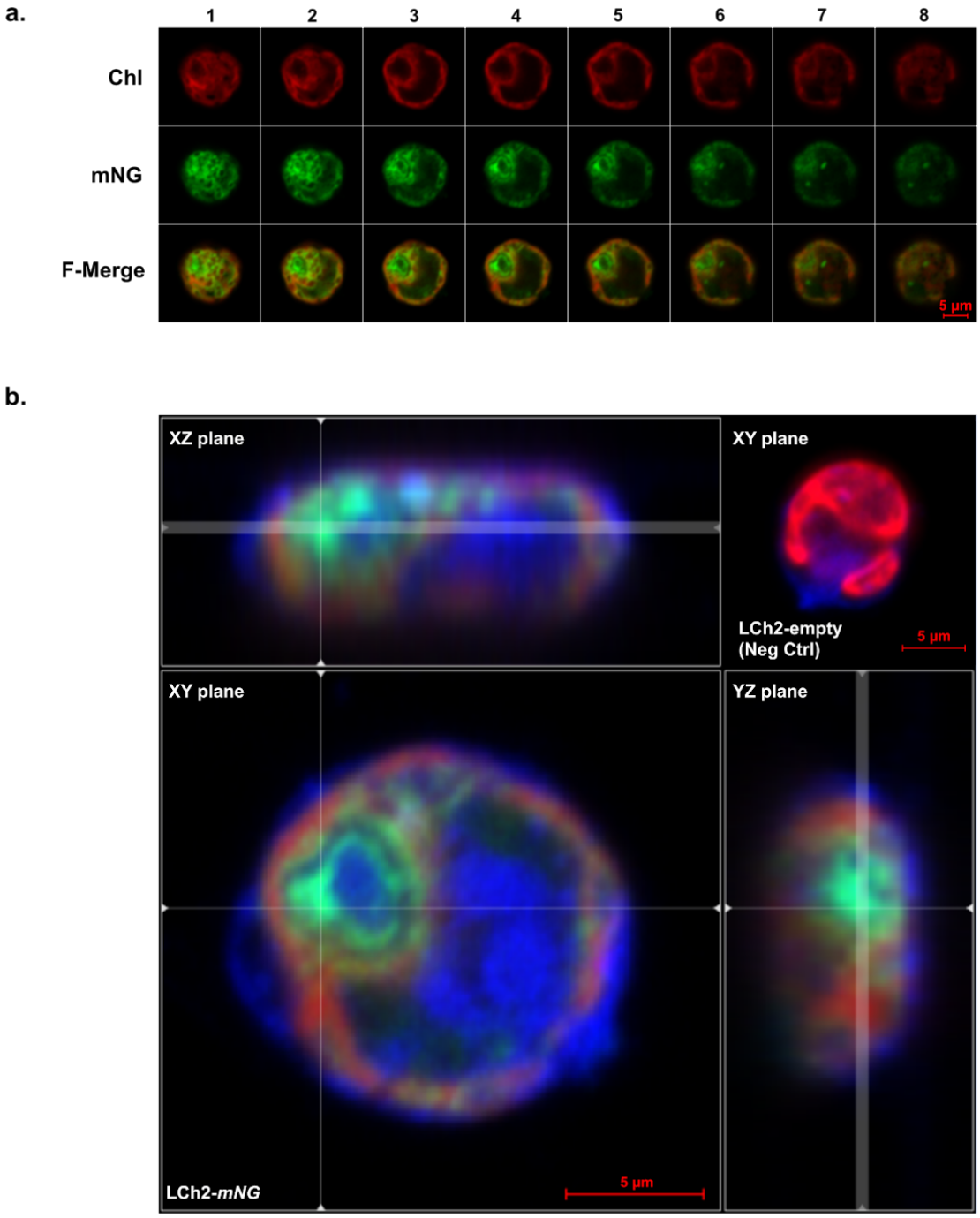

1123